

Significant Production of Ozone from Germicidal UV Lights at 222 nm

Zhe Peng,* Douglas A. Day, Guy A. Symonds, Olivia J. Jenks, Harald Stark, Anne V. Handschy, Joost A. de Gouw, and Jose L. Jimenez*



Cite This: *Environ. Sci. Technol. Lett.* 2023, 10, 668–674



Read Online

ACCESS |

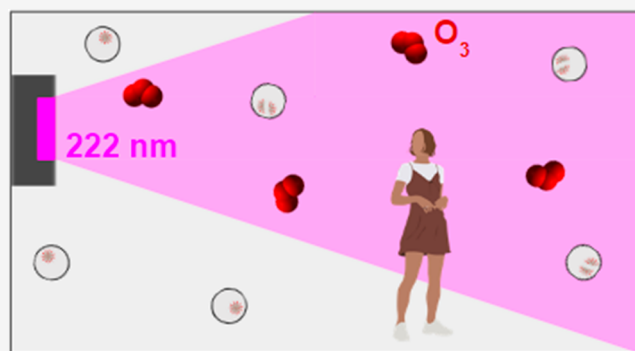
Metrics & More

Article Recommendations

Supporting Information

ABSTRACT: Lamps emitting at 222 nm have attracted recent interest for germicidal ultraviolet disinfection (“GUV222”). Their impact on indoor air quality is considered negligible. In this study, ozone formation is observed for eight different lamps from five manufacturers, in amounts an order of magnitude larger than previous reports. Most lamps produce O₃ in amounts close to the first-principles calculation, with, e.g., a generation rate of 22 ppb h⁻¹ for Ushio B1 modules in a 21 m³ chamber. Much more O₃ is produced by lamps when optical filters are removed for tests and by an undesired internal electrical discharge. A test in an office shows an increase of ~6.5 ppb during lamp-on periods, consistent with a simple model with the O₃ generation rate, ventilation, and O₃ losses. We demonstrate the use of a photolytic tracer (CBr₄) to quantify the averaged GUV222 fluence rate in a room. An important consequence of O₃ production by GUV222 is particulate matter (PM) formation, which may have significant negative health impacts. To limit GUV222-created indoor pollution, new guidelines should be developed and lower fluence rates should be used if possible, especially under low-ventilation conditions. Low-cost sensors for O₃ and PM were not useful for investigating GUV222-induced chemistry.

KEYWORDS: germicidal ultraviolet, far-UVC, ozone generation, indoor air quality, chemical actinometry, chamber experiment



1. INTRODUCTION

Germicidal ultraviolet (GUV) disinfection has been used for a century to inactivate airborne pathogens, i.e., those that infect via inhalation of pathogen-containing aerosols that float in the air.^{1–3} Despite some early interest in widespread deployment (e.g., a campaign from Westinghouse to install GUV lamps in every American home⁴), it has remained mostly a niche technique in medical circles, in particular to reduce tuberculosis transmission.⁵ Research during the COVID-19 pandemic led to the conclusion that airborne transmission is dominant for this virus⁶ and also important for other respiratory viruses.⁷ This has resulted in intense interest in methods to remove pathogens from the air, including ventilation, filtration, and air disinfection, in particular by GUV.⁸

GUV uses lamps that emit light in the UVC range (200–280 nm) to irradiate indoor air, which can inactivate aerosol-bound pathogens. It has traditionally been performed using filtered mercury lamps whose most intense emission is at 254 nm (“GUV254”). More recently, the use of shorter wavelengths (“far UVC”, 200–230 nm) has gained in popularity, in particular using KrCl excimer lamps with a peak emission of 222 nm (“GUV222”), because direct irradiation of humans is thought to be much safer than for GUV254.⁹ Extensive

scientific reference information on GUV has been compiled at the online GUV Cheat Sheet.¹⁰

UVC lamps with wavelengths below 242 nm can generate O₃,¹¹ a dangerous air pollutant. A recent review concluded that O₃ generation by KrCl excimer lamps was minimal: for example, a 12 W lamp was estimated to take 267 h to produce 4.5 ppb O₃ in a 30 m³ room in the absence of losses.¹² A recent modeling paper estimated O₃ generation to be nearly two orders of magnitude faster,¹³ but those findings have not been confirmed experimentally. There is also discussion in the literature whether O₃ is mainly formed by the UVC radiation or by discharges in electrical connections.¹²

In addition, it is typically difficult to quantify the GUV fluence rate that the air experiences in a room or chamber; since lamp emission results in inhomogeneous light spatial distributions, and the reflectivity of materials at the GUV wavelengths varies widely. Measurements in different points of

Received: May 14, 2023

Revised: July 12, 2023

Accepted: July 12, 2023

Published: July 28, 2023



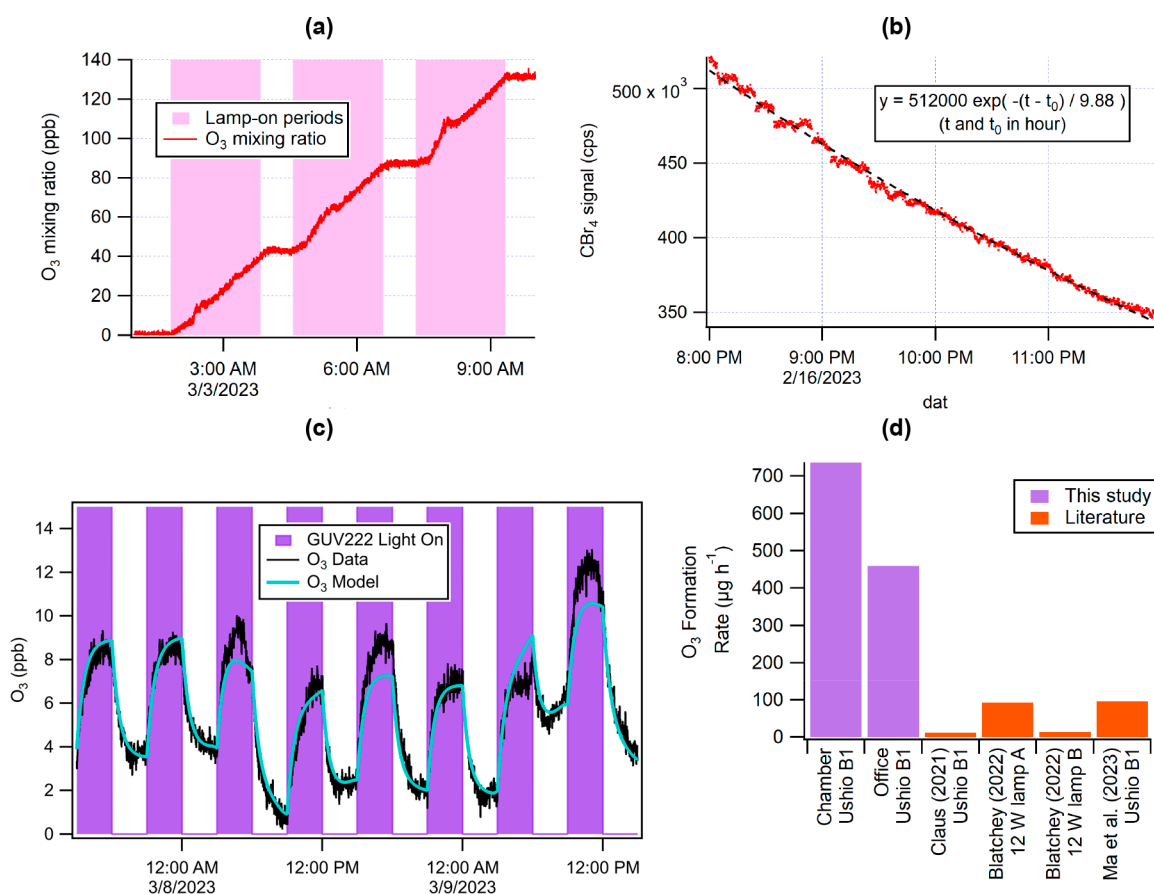


Figure 1. Time series of (a) O_3 during a “lamp on/off” chamber experiment and (b) CBr_4 during a continuous “lamp-on” experiment with the 12 W Far UV lamp (Ushio B1 module). (c) Time series of O_3 in the office experiments, along with model results. (d) Comparison of O_3 formation rates in this study with previous literature.

a room to quantify the average or computer modeling can be performed but are time-consuming. Quantification of the radiation field with measurements of inactivation of viruses or bacteria require culture assays which are slow and very costly.

Here, we present direct measurements of O_3 production from KrCl excimer lamps in a laboratory chamber and compare them with literature estimates. A chemical tracer that allows quantification of UV fluence rate is introduced. Measurements are also performed in an office. Significant O_3 production is observed in both controlled-laboratory and real-world settings.

2. METHODS

Demonstration of Tracers for UV Exposure of Air. In this work, we use CBr_4 as a chemical tracer of UV exposure. We show that it has relatively fast decay under 222 nm irradiation and can be detected by commonly available proton-transfer-reaction mass spectrometers with high sensitivity. It does not react with common atmospheric oxidants such as O_3 , OH, or NO_3 at typical indoor air concentrations. It has high vapor pressure and low water solubility which minimizes partitioning to room surfaces and tubing.^{14,15} More details can be found in section S1.

Laboratory Chamber Experiments. A well-characterized environmental chemical reaction chamber was used to measure the O_3 production rate and CBr_4 tracer decay for individual UV fixtures. A $\sim 21 \text{ m}^3$ Teflon reaction chamber (approximately $3 \times 3 \times 2 \text{ m}$, $L \times W \times H$) is constructed of 50- μm -

thick FEP Teflon film (ATEC, Malibu, California). Temperature during the experiments was $\sim 20\text{--}25 \text{ }^\circ\text{C}$, and the built-in chamber UVA/visible lights were not used other than at occasional low levels of visible lights for task lighting. The chamber systems are described in previous publications exploring chemical and physical processes of gases and aerosols.^{16,17} The UV light source was placed either a few centimeters outside the chamber (at one corner at $\sim 1 \text{ m}$ height shining into the bag and across the horizontal diagonal to the opposite corner) or placed within the chamber (at a corner on the bottom of the chamber bag mounted on a ring stand facing the opposite upper corner; Figure S1).

A typical experiment was conducted as follows. Prior to each experiment, the chamber was flushed for several hours with 400 LPM clean air ($\text{NO}_x < 0.2 \text{ ppb}$; $\text{VOC} < 50 \text{ ppb}$) from an AADCO generator (Model 737–15A; at slightly positive pressure, 1–2 Pa) and then topped off to consistently reach the full volume ($\sim 21 \text{ m}^3$) by filling until the differential pressure reached 3.5 Pa. The UV lamp was then turned on either continuously (Figure 1b) or on/off in steps (e.g., 120 min on, 45 min off, Figure 1a) for several hours. O_3 formation was measured with a Thermo Scientific 49i O_3 Analyzer. Later in the experiments while the UV lamp was off, several parts per billion of CBr_4 were added by placing the solid compound within a glass bulb and gently heating with a heat gun while flowing ultrahigh purity nitrogen gas (for $\sim 2 \text{ min}$) and then mixing for 1 min with a Teflon-coated mixing fan (integrated in the chamber). The on/off operation allowed to unequiv-

Table 1. KrCl Excimer Lamps Tested in the Chamber Experiments and Key Results^a

manufacturer	model	spectrum or lamp	inside or outside teflon bag?	filtered?	measured electrical power (W)	O ₃ generation rate (ppb h ⁻¹)	CBr ₄ photolysis rate (h ⁻¹)	ratio of O ₃ generation rate to CBr ₄ photolysis rate (ppb h ⁻¹ / (μW cm ⁻²))	O ₃ generated per unit power (μg h ⁻¹ W ⁻¹)	fluence rate ^b (μW cm ⁻²)	ratio of O ₃ generation rate to fluence rate (ppb h ⁻¹ / (μW cm ⁻²))
N/A		theoretical calculation w/ narrow emission line at 222 nm ^c				14	0.11	130		2.1	6.7
N/A		theoretical calc. w/ Ushio B1 (NIST-measured spectrum) ^c				22	0.097	230		2.1	10
N/A		theoretical calc. for unfiltered lamp (Ushio B1 NIST spectrum, adding an estimated 190 nm band) ^d				88	0.097	910		2.2	40
far UV	Krypton-36	Ushio B1	inside	yes	15	21	0.093	230	47	2.0	11
far UV	Krypton-36	Ushio B1	inside	no, removed by us	15	100	0.21	490	220	4.6	22
far UV	Krypton-36	Ushio B1	outside	no, removed by us		66					
custom	N/A	Ushio B1	inside	yes	16	23	0.10	230	48	2.2	10
custom	N/A	Ushio B1.5 (with diffuser)	inside	yes	11	8.5	0.051	170	26	1.1	7.7
Naomi Wu, China	N/A	GMV FAR-UVC 15 W	inside	yes	15	11	0.039	280	25	0.84	13
Naomi Wu, China (portable)	N/A	FIRST UVC HEXAGON - USB	inside	yes	5	2.0	0.0095	210	13	0.21	10
ERGO HealthTech	X One	not known	inside	yes	5	2.0	0.0081	250	13	0.18	11
Eden Park (A)	Pre-productionMobile-Shield ²²²	Eden Park Microplasma Far-UVC	inside	yes	9	30	0.030	1000	110	0.65	46
Eden Park (A)	Pre-productionMobile-Shield ²²²	Eden Park Microplasma Far-UVC	inside	no, removed by us	9	70	0.040	1800	260	0.86	81
Eden Park (A)	Pre-productionMobile-Shield ²²²	Eden Park Microplasma Far-UVC	outside	no, removed by us		0.51					
Eden Park (B)	Pre-productionMobile-Shield ²²²	Eden Park Microplasma Far-UVC	inside	yes	9	1.3	0.010	120	4.8	0.22	5.9
Eden Park (B)	Pre-productionMobile-Shield ²²²	Eden Park Microplasma Far-UVC	inside	no, removed by us	9	14	0.039	360	52	0.84	17

^aAlso shown are the results of first-principles calculations with different lamp spectra. ^bCalculated from CBr₄ photolysis rate under the assumption of a constant fluence rate for all the bag volume, and the same 222 nm band shape as the NIST-measured Ushio B1 spectrum. ^cHypothetical case with a total UV intensity of 2.3×10^{12} photons cm⁻² s⁻¹. ^dHypothetical case with the same 222 nm band as the NIST-measured Ushio B1 spectrum and an artificial 190 nm band, constructed from the spectrum shown in ref 12 (Figure S2).

ocally attribute changes in the O₃ and CBr₄ mixing ratios to the GUV illumination and to quantify any other losses separately. A Vocus Proton-Transfer-Reaction Mass Spectrometer (referred to as “Vocus” hereafter) measured CBr₄ (detected as CBr₃⁺). It was calibrated by adding a known quantity to the chamber.¹⁸ See sections S2 and S3 for more information on calibrations of the O₃ analyzers and Vocus.

Since a single lamp fixture was illuminating from one corner of the bag, the fluence rate is not constant within the bag volume. However, on the time scales of the experiments (relative to the production/decay of the measured compounds), the air within the chamber is relatively well mixed. This is due to the continuous mixing that occurs in the absence of mechanical mixing, with a time scale of ~10 min.¹⁷ This is apparent in the stepwise lamp illumination experiments, by the relatively quick stabilization of CBr₄ and O₃ when the light is turned off (Figure 1a).

Office Experiments. Experiments were also performed in a small university office, which measured 4.0 × 2.7 × 3.1 m (L × W × H; vol. ~ 33 m³). It has an entrance door and two windows. A supply and a return vent are located near the ceiling. To simulate a low-ventilation situation, the windows, gaps around utility penetrations, and supply/return vents were sealed with plastic sheeting or tape (Figure S3).

The ventilation rate was quantified by monitoring the decay of CO₂ after an injection (from a compressed gas cylinder) with an Aranet4 sensor (SAFTehnika, Latvia). A fan was turned on remotely for a few seconds after CO₂ injection to ensure homogeneity within the room. The ventilation/infiltration rate was estimated with an exponential fit to the CO₂ decay to be comparable to typical residences,¹⁹ but with some experiment-to-experiment variability. For this reason, CO₂ was injected also during the O₃ decay or production experiments.

To quantify the O₃ decay to surfaces and to gas and aerosol chemistry in the room, the O₃ decay in the room was measured with a 2B 205 analyzer. The decay was fit to an exponential, and the O₃ deposition rate coefficient was determined by subtracting the ventilation rate coefficient (Figure S4).

3. RESULTS

Theoretical Estimation of O₃ Production and Tracer Decay. In this study, we tested lamps from different manufacturers (Table 1). The emission spectrum of the Ushio B1 lamp that is used by multiple lamp manufacturers is available from NIST (Figure S2). The absorption spectra of O₂ and CBr₄ are well-known.^{11,20} Their expected photolysis rates under the Ushio B1 lamp irradiation can be calculated by integrating the product of UV fluence rate and absorption cross sections of O₂ or CBr₄ over the wavelengths of interest. As two molecules of O₃ are produced per O₂ molecule photolyzed, the theoretical O₃ production rate for the Ushio B1 lamp at an average UV fluence rate of 2.3 × 10¹² photons cm⁻² s⁻¹ is ~22 ppb h⁻¹. At the same UV intensity, the theoretical CBr₄ photolysis rate is 0.097 h⁻¹. The ratio between them (P_{O₃}/J_{CBr₄} ~ 230 ppb), i.e., O₃ production through O₂ photolysis over a period for an e-fold decay of CBr₄, is independent of UV fluence rate and is characteristic of a specific GUV222 lamp.

When unfiltered optically, the emission of the KrCl excimer lamp also includes a band centered at 190 nm (Figure S2).¹² If this band is added to the theoretical calculation (as a proxy of unfiltered lamps), the O₃ generation rate is increased by a

factor of ~4. Although the 190 nm band has much lower intensity, the absorption cross section of O₂ is on average ~2 orders of magnitude larger for the 190 nm band than for the 222 nm one. However, this band has little impact on CBr₄ as its cross section below 200 nm is much lower. This results in a higher P_{O₃}/J_{CBr₄} ratio (~900 ppb) than for the filtered lamp spectrum.

O₃ Production and CBr₄ in the Chamber. Results of a typical chamber experiment (Ushio B1) are shown in Figure 1a. O₃ increases approximately linearly with time when the lamp is on. When this lamp is on for an extended period (days), O₃ in the chamber can reach parts per million levels (Figure S5). At very high O₃ concentrations, the small loss rate coefficient of O₃ (mainly due to photolysis by the 222 nm band, Figure S6) slightly reduces the rate of O₃ increase, while losses to the walls remain negligible. An Ushio B1 lamp generates ~22 ppb O₃ per hour, very close to the theoretical case shown above. The UVC fluence rate inferred from the CBr₄ photolytic decay rate (~0.1 h⁻¹, dilution corrected, Table 1; Figure 1b) is also very close to the theoretical case value. P_{O₃}/J_{CBr₄}, a characteristic of the lamp, is almost the same as the theoretical case value (Table 1). A recent study showed excellent consistency between our actinometry measurements and spatially and spectrally resolved fluence rate measurements for the Ushio lamps.²¹

The other devices tested in this study, with electrical power ranging from ~5 W (portable device) to ~15 W, also have P_{O₃}/J_{CBr₄} values in the range of 200–300 ppb, indicating similar spectral characteristics of their emissions. The exceptions are the lamps whose filters were removed for our tests, two Eden Park lamps we tested, and an Ushio B1.5 lamp with a diffuser.

The Ushio B1 device with filter removed had 4 times higher O₃ production and >100% larger CBr₄ decay than when filtered, leading to ~110% higher P_{O₃}/J_{CBr₄}. Without the filter, more photons of the 222 nm band are allowed out of the device, leading to faster CBr₄ decay. The 190 nm band is also unfiltered, producing much more O₃ than the 222 nm band of the device with a filter can produce. The P_{O₃}/J_{CBr₄} of most lamps tested in this study are close to that of the NIST-measured Ushio B1 emission spectrum, indicating very minor importance of the 190 nm band in their filtered emissions.

The Eden Park lamp has almost the same emission spectrum as the Ushio B1 (Figure S7). With its filter, the first Eden Park device tested (EP-A, Table 1) results in ~1/3 CBr₄ decay vs Ushio B1, while producing more O₃. Most of this unexpectedly high O₃ production appears to be due to electrical discharge within the electrical components of the device (but outside the lamp). We arrive at this conclusion after additional tests: (i) low O₃ production by the EP-A in the chamber bag when located outside the bag, in contrast to the Ushio B1 module (Table 1). (ii) For O₃ measurement just outside the EP-A housing, but not in front of the light, the O₃ monitor detects parts-per-million-level O₃ (Figure S8), implying very strong nonphotochemical O₃ production inside the device. Eden Park indicated that the abnormal ozone production was a result of the electrical assembly in a pre-production unit, and that all commercial units meet UL/CARB requirements.

In contrast, the other Eden Park device test (EP-B) did not produce an excessive amount of O₃ in its housing, implying no undesired electrical discharge there. It also only produces 1.3 and 14 ppb O₃ per hour in the chamber with and without its filter, respectively, resulting in significantly lower P_{O₃}/J_{CBr₄}

than the Ushio B1 lamps. The reasons for the lower P_{O_3}/J_{CBR4} of the Ushio B1.5 module and EP-B lamp may be related to differences in spectral emission vs angle, due to the different filters used.²¹ Both lamps have similar emission spectra to that of Ushio B1 in the normal direction (Figure S7).

Finally, we note that O_3 production per unit electrical power is proportional to the efficiency of the lamp. The range of efficiencies of current lamps spans an order-of-magnitude.

O_3 Mass Balance in an Office. The Far UV lamp was repeatedly cycled on (3 h) and off (3 h) together with periodic CO_2 injections (Figure 1c and Figure S9). O_3 rapidly rose once the lamp was turned on and reached an approximate steady state (8–14 ppb, typically increasing ~ 6.5 ppb). After turning off the lamp, O_3 rapidly decreased, also quickly reaching a steady state. Background O_3 in the office, as indicated by the steady-state O_3 level at the end of lamp-off periods, varied by ~ 4 ppb during the experiment. It is affected by ventilation rate, deposition, as well as O_3 in outdoor/adjacent-room air infiltrating into the office. Ventilation rates ranged 0.62–0.96 h^{-1} (Figure S9). O_3 deposition rates were more variable (range 0.5–2.3 h^{-1} , average 0.78 h^{-1} , Figure S9).

O_3 in the office was modeled with a chemical-kinetics simulator.²² The model was constrained by the measured O_3 and CO_2 concentrations and decays (section S4). The measured and modeled O_3 are in good agreement (Figure 1c). The O_3 production rate of the Ushio B1 module in the office (Figure S3) is estimated to be 8.6 ppb/h from the constrained model. This is $\sim 41\%$ of the value measured in the chamber, which is explained by the larger volume of the office (~ 32.9 vs ~ 20.6 m^3) and the shorter effective UV path length (~ 3.2 vs ~ 4.5 m). Scaling results in a difference of 8%, thus showing agreement well within experimental uncertainties (Figure S10).

Implications. Significant amounts of O_3 can be produced by GUV-222 lamps in both controlled-laboratory and real-world settings. Our results of 736 μg h^{-1} for a 20.6 m^3 chamber and 459 μg h^{-1} for an office with a shorter light path from an Ushio B1 module are summarized in Figure 1d. Note that these results would be $\sim 21\%$ higher at sea level due to the reduced ambient pressure in Boulder. For comparison, previous reports for the same GUV222 module (or modules using the same electrical power) from the literature of 12,¹² 13 and 92,⁹ and 96 μg h^{-1} ²³ are also shown. These had been used to conclude that O_3 generation from GUV222 is not a concern. On average, our results are an order of magnitude larger than the literature. The discrepancy may arise because most prior measurements were performed in small boxes, with very short optical pathlengths and high surface/volume ratios that are not representative of real room applications. The former may lead to a smaller O_3 production rate and the latter to substantial losses to the box surfaces, which were not accounted for. Moreover, some of these measurements may have been made with low-cost electrochemical O_3 sensors. We tested several low-cost O_3 and PM sensors and did not find them to be useful for GUV222-induced indoor air chemistry studies (section S5).

O_3 itself is a major air pollutant causing excess deaths at levels below those in occupational guidelines of 50–100 ppb.^{24,25} More importantly, it can also lead to formation of other pollutants including particulate matter,¹³ whose excess death impacts can be many times higher than those of O_3 itself (section S6).^{24,26} O_3 production by GUV222 lamps thus can be a major concern, at least under low-ventilation conditions.

Our Ushio B1 experiments have an average fluence rate of ~ 2.1 μW cm^{-2} , about 1/3 of the recently updated American Conference of Governmental Industrial Hygienists (ACGIH) eye limit, and somewhat higher than the typical upper limit of the room-average fluence rate for a room installation that complies with the ACGIH eye limit (0.3–1.5 μW cm^{-2} , H. Claus, personal communication). ACGIH and other organizations should consider additional GUV222 fluence rate limits and related guidelines (e.g., CO_2 monitoring and alarming to detect low ventilation conditions) to specifically address GUV222 indoor air quality impacts. Current literature estimates of the GUV222 disinfection rate coefficient for SARS-CoV-2 span a factor of 8.4.^{27–29} Future research should focus on narrowing down this range, which may allow high efficacy of GUV222 at lower fluences, thus reducing impacts on indoor air.

■ ASSOCIATED CONTENT

Supporting Information

The Supporting Information is available free of charge at <https://pubs.acs.org/doi/10.1021/acs.estlett.3c00314>.

Absorption (emission) spectra of key species (a few lamps) and details about tracer selection, chamber experiments, analysis and modeling of the office experiment, low-cost sensor evaluations for this application, and relative health effect estimation for O_3 vs PM. (PDF)

■ AUTHOR INFORMATION

Corresponding Authors

Zhe Peng – Department of Chemistry, University of Colorado, Boulder, Colorado 80309, United States; Cooperative Institute for Research in Environmental Sciences (CIRES), University of Colorado, Boulder, Colorado 80309, United States; orcid.org/0000-0002-6823-452X; Email: zhe.peng@colorado.edu

Jose L. Jimenez – Department of Chemistry, University of Colorado, Boulder, Colorado 80309, United States; Cooperative Institute for Research in Environmental Sciences (CIRES), University of Colorado, Boulder, Colorado 80309, United States; orcid.org/0000-0001-6203-1847; Email: jose.jimenez@colorado.edu

Authors

Douglas A. Day – Department of Chemistry, University of Colorado, Boulder, Colorado 80309, United States; Cooperative Institute for Research in Environmental Sciences (CIRES), University of Colorado, Boulder, Colorado 80309, United States; orcid.org/0000-0003-3213-4233

Guy A. Symonds – Department of Chemistry, University of Colorado, Boulder, Colorado 80309, United States; Cooperative Institute for Research in Environmental Sciences (CIRES), University of Colorado, Boulder, Colorado 80309, United States

Olivia J. Jenks – Department of Chemistry, University of Colorado, Boulder, Colorado 80309, United States; Cooperative Institute for Research in Environmental Sciences (CIRES), University of Colorado, Boulder, Colorado 80309, United States; orcid.org/0000-0002-4184-3296

Harald Stark – Department of Chemistry, University of Colorado, Boulder, Colorado 80309, United States; Cooperative Institute for Research in Environmental Sciences

(CIRES), University of Colorado, Boulder, Colorado 80309, United States; Aerodyne Research, Billerica, Massachusetts 01821, United States; orcid.org/0000-0002-0731-1202

Anne V. Handschy – Department of Chemistry, University of Colorado, Boulder, Colorado 80309, United States; Cooperative Institute for Research in Environmental Sciences (CIRES), University of Colorado, Boulder, Colorado 80309, United States

Joost A. de Gouw – Department of Chemistry, University of Colorado, Boulder, Colorado 80309, United States; Cooperative Institute for Research in Environmental Sciences (CIRES), University of Colorado, Boulder, Colorado 80309, United States; orcid.org/0000-0002-0385-1826

Complete contact information is available at:

<https://pubs.acs.org/10.1021/acs.estlett.3c00314>

Notes

The authors declare no competing financial interest.

This paper has been previously submitted to medRxiv, a preprint server for health sciences. The preprint can be cited as Peng, Z.; Day, D. A.; Symonds, G.; Jenks, O.; Stark, H.; Handschy, A. V.; de Gouw, J.; Jimenez, J. L. Significant Production of Ozone from Germicidal UV Lights at 222 nm. *medRxiv* **2023**, DOI: 10.1101/2023.05.13.23289946.

ACKNOWLEDGMENTS

We thank the Balvi Filantropic Fund, the CIRES Innovative Research Program, and the Sloan Foundation (grant 2019-12444) for support of this work. We thank Shelly Miller, Kenneth Wood, Ewan Eadie, Catherine Noakes, Dustin Poppendieck, Michael Link, Mikael Ehn, Jesse Kroll, Victoria Barber, John Balmes, Sung-Jin Park and the larger GUV scientific and technical communities for useful discussions and Melissa Morris for assistance in experiments. We are grateful to Holger Claus, Aaron Collins, Matthew Pang, Kristina Chang, Scott Diddams, and Naomi Wu for sharing data or materials and useful discussions.

REFERENCES

- (1) Wells, W. F. Air Disinfection in Day Schools. *Am. J. Public Health Nations. Health* **1943**, *33* (12), 1436–1443.
- (2) Riley, R. L.; Mills, C. C.; O'grady, F.; Sultan, L. U.; Wittstadt, F.; Shivpuri, D. N. Infectiousness of Air from a Tuberculosis Ward. Ultraviolet Irradiation of Infected Air: Comparative Infectiousness of Different Patients. *Am. Rev. Respir. Dis.* **1962**, *85*, 511–525.
- (3) Nardell, E. A. Air Disinfection for Airborne Infection Control with a Focus on COVID-19: Why Germicidal UV Is Essential. *Photochem. Photobiol.* **2021**, *97* (3), 493–497.
- (4) Fitzgerald, G. *The Origins of Aerobiology and Airborne Disease Research in the United States, 1930–1955*; Intervals Podcast of the Organization of American Historians, June 30, 2021. <https://rebrand.ly/m0uxwym>.
- (5) Mphaphlele, M.; Dharmadhikari, A. S.; Jensen, P. A.; Rudnick, S. N.; van Reenen, T. H.; Pagano, M. A.; Leuschner, W.; Sears, T. A.; Milonova, S. P.; van der Walt, M.; Stoltz, A. C.; Weyer, K.; Nardell, E. A. Institutional Tuberculosis Transmission. Controlled Trial of Upper Room Ultraviolet Air Disinfection: A Basis for New Dosing Guidelines. *Am. J. Respir. Crit. Care Med.* **2015**, *192* (4), 477–484.
- (6) Greenhalgh, T.; Jimenez, J. L.; Prather, K. A.; Tufekci, Z.; Fisman, D.; Schooley, R. Ten Scientific Reasons in Support of Airborne Transmission of SARS-CoV-2. *Lancet* **2021**, *397*, 1603–1605.
- (7) Wang, C. C.; Prather, K. A.; Sznitman, J.; Jimenez, J. L.; Lakdawala, S. S.; Tufekci, Z.; Marr, L. C. Airborne Transmission of Respiratory Viruses. *Science* **2021**, *373* (6558), No. eabd9149.
- (8) Morawska, L.; Tang, J. W.; Bahnfleth, W.; Bluyssen, P. M.; Boerstra, A.; Buonanno, G.; Cao, J.; Dancer, S.; Floto, A.; Franchimon, F.; Haworth, C.; Hogeling, J.; Isaxon, C.; Jimenez, J. L.; Kurnitski, J.; Li, Y.; Loomans, M.; Marks, G.; Marr, L. C.; Mazzarella, L.; Melikov, A. K.; Miller, S.; Milton, D. K.; Nazaroff, W.; Nielsen, P. V.; Noakes, C.; Peccia, J.; Querol, X.; Sekhar, C.; Seppänen, O.; Tanabe, S.-I.; Tellier, R.; Tham, K. W.; Wargocki, P.; Wierzbicka, A.; Yao, M. How Can Airborne Transmission of COVID-19 Indoors Be Minimised? *Environ. Int.* **2020**, *142*, 105832.
- (9) Blatchley, E. R.; Brenner, D. J.; Claus, H.; Cowan, T. H.; Linden, K. G.; Liu, Y.; Mao, T.; Park, S.-J.; Piper, P. J.; Simons, R. M.; Sliney, D. H. Far UV-C Radiation: An Emerging Tool for Pandemic Control. *Crit. Rev. Environ. Sci. Technol.* **2023**, *53* (6), 733–753.
- (10) Jimenez, J. L. GUV Cheat Sheet. <http://bit.ly/guv-cheat>.
- (11) Burkholder, J. B.; Sander, S. P.; Abbott, J.; Barker, J. R.; Cappa, C.; Crouse, J. D.; Dibble, T. S.; Huie, R. E.; Kolb, C. E.; Kurylo, M. J.; Orkin, V. L.; Percival, C. J.; Wilmouth, D. M.; Wine, P. H. *Chemical Kinetics and Photochemical Data for Use in Atmospheric Studies*; JPL Publication 19–5; Jet Propulsion Laboratory: Pasadena, 2019.
- (12) Claus, H. Ozone Generation by Ultraviolet Lamps†. *Photochem. Photobiol.* **2021**, *97* (3), 471–476.
- (13) Peng, Z.; Miller, S. L.; Jimenez, J. L. Model Evaluation of Secondary Chemistry due to Disinfection of Indoor Air with Germicidal Ultraviolet Lamps. *Environ. Sci. Technol. Lett.* **2023**, *10* (1), 6–13.
- (14) Pagonis, D.; Price, D. J.; Algrim, L. B.; Day, D. A.; Handschy, A. V.; Stark, H.; Miller, S. L.; de Gouw, J.; Jimenez, J. L.; Ziemann, P. J. Time-Resolved Measurements of Indoor Chemical Emissions, Deposition, and Reactions in a University Art Museum. *Environ. Sci. Technol.* **2019**, *53* (9), 4794–4802.
- (15) Liu, X.; Deming, B.; Pagonis, D.; Day, D. A.; Palm, B. B.; Talukdar, R.; Roberts, J. M.; Veres, P. R.; Krechmer, J. E.; Thornton, J. A.; de Gouw, J. A.; Ziemann, P. J.; Jimenez, J. L. Effects of Gas-wall Interactions on Measurements of Semivolatile Compounds and Small Polar Molecules. *Atmos. Meas. Tech.* **2019**, *12* (6), 3137–3149.
- (16) Liu, X.; Day, D. A.; Krechmer, J. E.; Brown, W.; Peng, Z.; Ziemann, P. J.; Jimenez, J. L. Direct Measurements of Semi-Volatile Organic Compound Dynamics Show near-Unity Mass Accommodation Coefficients for Diverse Aerosols. *Commun. Chem.* **2019**, *2*, 98.
- (17) Krechmer, J. E.; Day, D. A.; Ziemann, P. J.; Jimenez, J. L. Direct Measurements of Gas/Particle Partitioning and Mass Accommodation Coefficients in Environmental Chambers. *Environ. Sci. Technol.* **2017**, *51* (20), 11867–11875.
- (18) Krechmer, J.; Lopez-Hilfiker, F.; Koss, A.; Hutterli, M.; Stoermer, C.; Deming, B.; Kimmel, J.; Warneke, C.; Holzinger, R.; Jayne, J.; Worsnop, D.; Fuhrer, K.; Gonin, M.; de Gouw, J. Evaluation of a New Reagent-Ion Source and Focusing Ion–Molecule Reactor for Use in Proton-Transfer-Reaction Mass Spectrometry. *Anal. Chem.* **2018**, *90* (20), 12011–12018.
- (19) Nazaroff, W. W. Residential Air-Change Rates: A Critical Review. *Indoor Air* **2021**, *31* (2), 282–313.
- (20) Keller-Rudek, H.; Moortgat, G. K.; Sander, R.; Sørensen, R. *MPI-Mainz UV/VIS Spectral Atlas of Gaseous Molecules of Atmospheric Interest*. http://satellite.mpic.de/spectral_atlas (accessed February 10, 2022).
- (21) Bergman, R. S. Goniophotometric Intensity and Spectral Measurements in the UV of a Care222 Excimer Lamp Unit with and without a Filter and Diffuser Unit. In *First International Congress on Far-UVC Science and Technology*; Columbia University, New York City, June 14–16, 2023.
- (22) Peng, Z.; Jimenez, J. L. KinSim: A Research-Grade, User-Friendly, Visual Kinetics Simulator for Chemical-Kinetics and Environmental-Chemistry Teaching. *J. Chem. Educ.* **2019**, *96* (4), 806–811.
- (23) Ma, B.; Burke-Bevis, S.; Tiefel, L.; Rosen, J.; Feeney, B.; Linden, K. G. Reflection of UVC Wavelengths from Common Materials during Surface UV Disinfection: Assessment of Human UV Exposure and Ozone Generation. *Sci. Total Environ.* **2023**, *869*, 161848.

(24) Turner, M. C.; Jerrett, M.; Pope, C. A., 3rd; Krewski, D.; Gapstur, S. M.; Diver, W. R.; Beckerman, B. S.; Marshall, J. D.; Su, J.; Crouse, D. L.; Burnett, R. T. Long-Term Ozone Exposure and Mortality in a Large Prospective Study. *Am. J. Respir. Crit. Care Med.* **2016**, *193* (10), 1134–1142.

(25) Bell, M. L.; Peng, R. D.; Dominici, F. The Exposure-response Curve for Ozone and Risk of Mortality and the Adequacy of Current Ozone Regulations. *Environ. Health Perspect.* **2006**, *114* (4), 532–536.

(26) Weichenthal, S.; Pinault, L.; Christidis, T.; Burnett, R. T.; Brook, J. R.; Chu, Y.; Crouse, D. L.; Erickson, A. C.; Hystad, P.; Li, C.; Martin, R. V.; Meng, J.; Pappin, A. J.; Tjepkema, M.; van Donkelaar, A.; Weagle, C. L.; Brauer, M. How Low Can You Go? Air Pollution Affects Mortality at Very Low Levels. *Sci. Adv.* **2022**, *8* (39), No. eabo3381.

(27) Ma, B.; Gundy, P. M.; Gerba, C. P.; Sobsey, M. D.; Linden, K. G. UV Inactivation of SARS-CoV-2 across the UVC Spectrum: KrCl* Excimer, Mercury-Vapor, and Light-Emitting-Diode (LED) Sources. *Appl. Environ. Microbiol.* **2021**, *87* (22), No. e0153221.

(28) Welch, D.; Buonanno, M.; Buchan, A. G.; Yang, L.; Atkinson, K. D.; Shuryak, I.; Brenner, D. J. Inactivation Rates for Airborne Human Coronavirus by Low Doses of 222 Nm Far-UVC Radiation. *Viruses* **2022**, *14* (4), 684.

(29) Robinson, R. T.; Mahfooz, N.; Rosas-Mejia, O.; Liu, Y.; Hull, N. M. UV222 Disinfection of SARS-CoV-2 in Solution. *Sci. Rep.* **2022**, *12* (1), 14545.